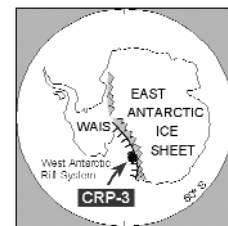


## Authigenic Smectite Clay Coats in CRP-3 Drillcore, Victoria Land Basin, Antarctica, as a Possible Indicator of Fluid Flow: A Progress Report

S.W. WISE, JR.<sup>1\*</sup>, J. SMELLIE<sup>2</sup>, F. AGHIB<sup>3</sup>, R. JARRARD<sup>4</sup> & L. KRISSEK<sup>5</sup><sup>1</sup>Department of Geological Sciences 4100, Florida State University, Tallahassee, FL 32306-4100 - USA<sup>2</sup>British Antarctic Survey, High Cross, Madingley Road, Cambridge CB3 0ET - UK<sup>3</sup>Dipartimento di Scienze della Terra, Università degli Studi di Milano, Via Mangiagalli 34, 20133 Milano - Italy<sup>4</sup>Department of Geology and Geophysics, University of Utah, Salt Lake City, Utah 84112 - USA<sup>5</sup>Department of Geological Sciences, Ohio State University, Columbus, Ohio 43210 - USA*Received 23 January 2001; accepted in revised form 13 November 2001*

**Abstract** - The presence of authigenic smectite in the lower Oligocene sandstones of the Cape Roberts Project core CRP-3 from the Victoria Land Basin of Antarctica is confirmed by scanning electron, scanning-transmission electron, and light microscopy. It was emplaced as a single generation of cement within the lower portion of the Oligocene section. This section has undergone no discernible compaction since cementation. Permeabilities measured on fifty core plugs show that the lower portion of the Oligocene (from 370-766 meters below sea floor) also has systematically higher values than sediment in uppermost CRP-3 and all of CRP-2 and CRP-1.

Three models for smectite authigenesis are considered as multiple working hypotheses to be tested: 1) Burial diagenesis with necessary components sourced from volcanogenic materials and heavy minerals within the drilled sequence; 2) Precipitation from hydrothermal waters associated with possible igneous intrusion(s) and nearby faults; 3) Mobilization and injection of regionally compactive "thermobaric" fluids along a nearby fault that bounds a major graben parallel to the Transantarctic Mountain Front. The preponderance of the available evidence and Occum's Razor favors the first model, although special circumstances dictated by the position of the drill site along a rapidly subsiding rift basin require that all three models be considered equally until our analyses are complete.



### INTRODUCTION

The third and final year of drilling at Cape Roberts on the western margin of the West Antarctic Rift System (Victoria Land Basin) in Antarctica (Fig. 1) produced a 940-m core at Site CRP-3 located in 295 m of water downslope from previously cored sites CRP-1 and CRP-2 to the east. At CRP-3, Neogene glacial erosion controlled by coast-parallel faulting associated with the Transantarctic Mountain (TAM) Front had removed overlying units (Cape Roberts Science Team, 1998), making older strata accessible for coring.

The core (Fig. 2) consists primarily of lower Oligocene and possibly some uppermost Eocene siliciclastic glacio-marine sediments deposited in a nearshore, cold-temperate to periglacial setting (Cape Roberts Science Team, 2000). The Cenozoic strata have been divided into 15 major lithologic units separated by an unconformity at 823.11 meters below seafloor (mbsf) from the subjacent Devonian Beacon Supergroup sandstones. Minor fault zones were identified or suspected to occur at 257-263, 539 and 790-801.5 mbsf. A highly altered 19-m-thick intrusion

within the Beacon sandstones (Lithologic Unit 17.1) is thought to represent Ferrar Supergroup dolerite (Cape Roberts Science Team, 2000). No pore-water samples were taken.

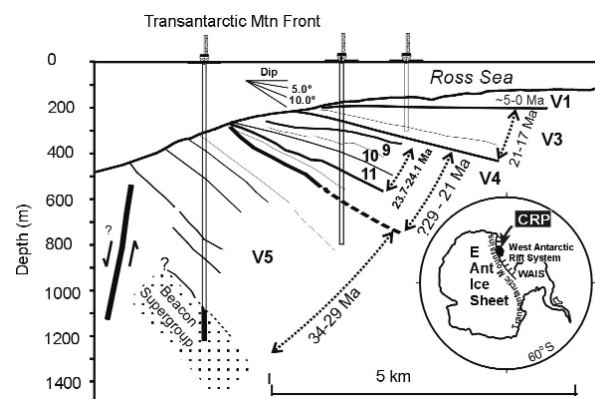


Fig. 1 - Map location of Cape Roberts drill sites, East Antarctic Ice Sheet, the Transantarctic Mountains, and the West Antarctic Rift System (which includes the Victoria Land Basin along its western margin). The interpreted seismic reflection profile shows CRP-1, CRP-2 and CRP-3, ages, and a fault in bold that bounds a graben to the west (from Cape Roberts Science Team, 2000, Fig. 1.4).

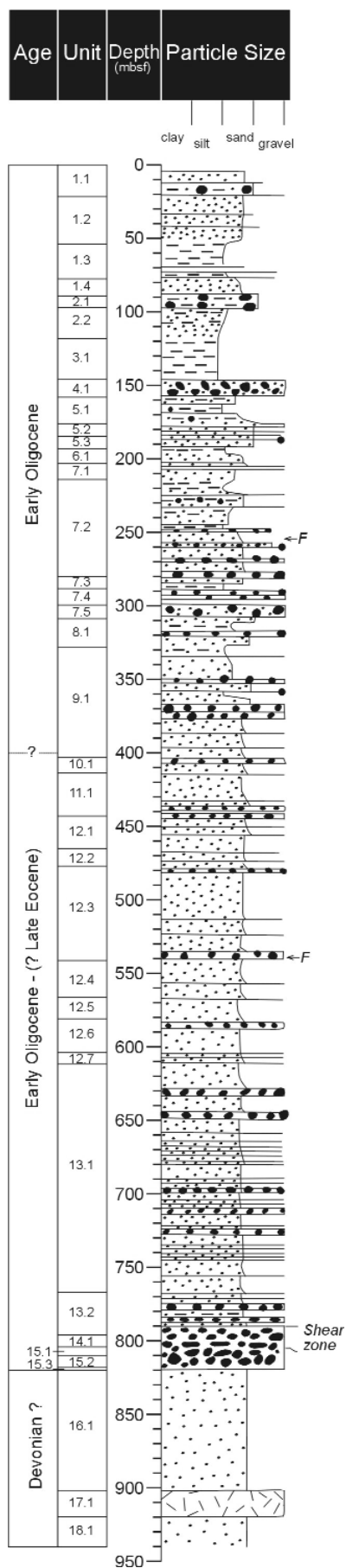


Fig. 2 - Stratigraphic column for CRP-3, showing main lithological features, faults, and ages. Ages are from Cape Roberts Science Team (2000).

During core processing at the Crary Science and Engineering Center (CSEC), McMurdo Station, Antarctica, an unusual greenish colour was noted in sandstones between 540 and 789.77 mbsf (Cape Roberts Science Team, 2000). In routine thin-section and nanofossil smear-slide preparations, these appeared to coat the sand grains and to display a “box-work” or “honey-comb” structure reminiscent of some authigenic clay minerals. Concurrent x-ray analysis conducted on site indicated that the clay mineral in question is smectite (Cape Roberts Science Team, 2000, Tab. 4.5; see discussion below). Independent shore-based grain-size and clay-mineralogy studies have also suggested respectively that diagenetic clay or authigenic smectite is present in portions of the core (see Barrett; Ehrmann; and Setti et al, all this volume). No such clays had been detected or suspected in the CRP-1, CRP-2, or CIROS-1 cores, where high concentrations of smectite have been attributed to changes of source area or climate (Cape Roberts Science Team, 1999; Ehrmann, 1997, 1998a, b). If the above observations on CRP-3 are correct, however, the presence of authigenic smectite might be the result of: 1) burial diagenesis, 2) hydrothermal activity, or 3) fault-focused compactive fluid flow through the rock at some stage in its history.

In the present study, we have conducted a preliminary survey of CRP-3 core using the scanning electron microscope (SEM), scanning transmission electron microscope (STEM), and light microscope (LM) in order to ascertain the morphology and probable extent of the clay mineral phase in question. In doing so, we have also recorded the presence of any authigenic calcite cement, which occurs extensively in portions of the core (Cape Roberts Science Team, 2000). In addition, we have made porosity and permeability measurements on selected core samples. Our ultimate goal in characterizing these various aspects of the core is to determine the origin and source of the smectite clay coatings on sandstone grains, and whether or not the rock has been subjected to heating and fluid flow during its history. A complete study will require more analyses than we have been able to run at the time of this writing. Thus, this contribution should be considered a progress report on an ongoing study.

## PREVIOUS WORK

### AUTHIGENIC CLAY MINERALS

Clay coats on sandstone grains, also referred to variously in the literature as clay coatings, clay rims, and pore-lining clays, may have a variety of allogenic or authigenic origins (Pittman et al., 1992). Authigenic clay coats, the primary object of the present study, may originate by direct precipitation

from formation waters (neof ormation) or through reactions between precursor materials and the pore fluids (regeneration). Such authigenic clay minerals are characterized by a radial morphology, euhedral crystal shape, and a high degree of crystallinity and purity (Wilson & Pittman, 1977; Hathon & Houseknecht, 1992). Purity may be reflected by their chemical composition, x-ray diffraction pattern, a uniformity of color and texture, and by their transparency. Indeed, some authigenic clays are monomineralic (Almon et al., 1976; Wilson & Pittman, 1977).

Because of their potential detrimental or beneficial effects on sandstone hydrocarbon reservoir quality, clay coats have been studied extensively during the past three decades, with comprehensive summaries provided by Wilson & Pittman (1977) and Pittman et al. (1992). Of the authigenic clay minerals found in sandstone reservoirs, smectite, glauconite, and kaolinite are found at the shallowest burial depths. These minerals, however, are likely to be joined or replaced at greater depths by other minerals such as mixed-layer smectite/chlorite, smectite/illite (= 10/17Å clay), dickite, chlorite, and illite, which form under conditions of greater heat and pressure.

For instance, outcrop samples of the Lower Cretaceous Woodbine Sandstone of Arkansas and shallow subsurface samples of its down-dip equivalent, the Tuscaloosa Sandstone, have authigenic smectite coats of uniform thickness, as do those in cores at depths as great as 1,676 m in the Big Creek Field of Louisiana (Pittman et al., 1992). Deeper cores at 2,371 m in nearby Tensas Parish, however, have chlorite coats. Cores to show the transition from smectite to chlorite are not available; however, Wilson & Pittman (1992, p. 247) suggest that such a transition would likely involve a mixed-layer chlorite/smectite phase. Similar examples have been noted from the Jurassic of the North Sea where early diagenetic clay-mineral assemblages (kaolinite, smectite and chlorites) dominated by kaolinite and detrital illitic/smectitic materials are found commonly in basin margin sandstones, and authigenic smectites are present only in the shallower reservoirs of the basin (see Burley & MacQuaker, 1992, and references therein).

It should be noted that depositional environment may in some cases provide an important control on the development of smectite vis a vis chlorite and corrensite (a mixed layer chlorite/smectite). Almon et al. (1976) found the occurrences of these two phases to be mutually exclusive in the Horsethief Formation of Wyoming. There, smectite precipitated in near-shore marine facies where the Mg/Ca ratios in initial pore fluids were lower relative to those in delta distributary channels and distributary mouth bars, in which corrensite developed (see Pittman et al., 1992, for several other such examples).

Silica concentration and temperature are also important factors in determining which authigenic

clay mineral will precipitate. Smectite authigenesis, like that of opal-CT and some zeolites, occurs below about 70° C. On the other hand, at temperatures above 60° C to 80° C, quartz precipitates more readily and smectite, no longer stable relative to pore fluids, begins to convert to illite (Bjørlykke & Aagaard, 1992, citing Aagaard & Helgeson, 1983 and Sass et al., 1987).

As to minimal temperatures for authigenesis in marine environments, several geologically young authigenic minerals can form in surface or near-surface environments. These include opal-CT in Pliocene sediments rich in biogenic silica of the Southern Ocean (Bormann et al. 1994) as well as Quaternary glauconite pellets and a variety of related Fe-rich clays and smectites in the Gulf of Guinea (Odin, 1988).

It is often stated that volcanic glass is unstable in marine environments and is rapidly replaced by other minerals or dissolves completely (*e.g.* Sturesson, 1992). Davies & Almon (1979; see also Davies et al., 1979) found that diagenesis of volcanic sands derived from modern subaerial andesitic eruptions in Guatemala can proceed quite rapidly (tens to hundreds of years) in both marine and non-marine environments under near-surface conditions; hematite-goethite, smectite, and zeolite are the principal cements they reported.

Clay authigenesis can also proceed relatively rapidly in deeply buried sandstone reservoirs once the necessary conditions are achieved. Comparative studies of a Miocene quartz/subarkosic sandstone in Sumatra subjected to different burial/temperature regimes due to faulting showed that kaolinite, illite and chlorite precipitated in only 1 to 2 m.y. when subjected to temperatures of 120-155° C and burial depths of about 1400 m. These clays were not precipitated, however, at shallower depths (about 800 m) where temperatures are about 70° C (Gluyas & Oxtoby, 1995, fig. 8).

The ultramorphology of authigenic smectite has been studied where it has replaced or precipitated within vesicles of subaerially erupted, Cenozoic rhyolitic materials to form clay deposits, such as the Ponza bentonite in Italy (Wise & Weaver, 1979; see also Lombardi & Mattias, 1981) or the Kinny Bentonite in Nevada (Khoury & Eberl, 1979; Wise & Ausburn, 1980). In both cases it developed as a honey-comb or box-work pattern of individual crystals. This pattern was also noted in previous studies of volcanoclastic sandstones (Almon et al., 1976; Wilson & Pittman, 1977).

Volcanic precursor materials figure prominently in most other reports of authigenic smectites such as in the aforementioned Woodbine Sandstone, a volcanic arenite with less than 10% quartz, and the Tuscaloosa Sandstone of Louisiana (Pittman et al., 1992). The Woodbine Sandstone contains trachytic and alkalic igneous lithic fragments, oligoclase feldspar, and Ti-rich pyroxenes.

Widespread upper Tertiary andesitic detritus from the Sierra Nevada Mountains was the source of thick, wax-like authigenic smectite coats that give volcanic arenites of the Mehrten Fm of California a distinctive blue color and translucent luster; some of the thicker coats consist of two layers (generations) of radial crystallites (Lerbekmo, 1957). Chemically pure with an unusual composition between beidellite and nontronite, these cements are equally common in both marine and non-marine facies, suggesting that the volcanoclastics and not pore-water composition controlled the mineral growth. Rhyolitic eruptions and the erosion of crystalline rocks of the Rocky Mountains were the primary sources of vitric and arkosic sandstones of the Cenozoic High Plains sequence, a semiarid alluvial and eolian complex of the mid-continent USA, in which smectite coats developed at low temperatures (10-30° C) and pressures (*c.* 1 bar) (Stanley & Benson, 1979).

Another notable example of volcanic material altering to smectite is the lower Tertiary tuffaceous sediments of the Bader Formation in the North Sea, which is composed mostly of altered volcanic ash and siliceous microfossils (Bjørlykke & Aagaard, 1992). Smectite occurs along with mixed-layer clays and chlorite. Bjørlykke & Aagaard (1992) suggest that the amorphous biogenic silica plus unstable Fe- and Mg-rich minerals in the volcanic debris served as precursors for the smectite and chlorite.

Many, but not all, authigenic clay mineral species have been synthesized in the laboratory from gels or precursor materials at elevated temperatures and pressures (*e.g.* Eberl & Hower, 1976; Whitney, 1990). Most pertinent to the present study are those precipitated experimentally within sandstones (*e.g.* Small et al., 1992a, b, Pittman et al., 1992), as these have demonstrated not only the mechanism by which such authigenic clay coats form, but also have allowed for controls on clay morphology, mineral stability, and mineralogy. Studies by Small et al. (1992a) show that the authigenic clays in sandstones are direct precipitates from solution that do not require a preexisting clay coating.

Pittman et al. (1992), who grew smectite coats on sand grains in a hydrothermal reactor, defined four stages in the experimental development of the clay coats. As they illustrated (Pittman et al., 1992, fig. 19), the process begins with the formation of isolated clay wisps in random orientation followed by the coalescence of these discrete clay platelets to form a non-porous "root system" tangential to the grain surface. From there the clay platelets grow primarily tangential to the grain surface to form a microporous, polygonal box-work pattern that infills to become denser while remaining only one-layer thick by the final growth stage. These authors not only noted similar morphologies in natural sandstones, but suggested that the flatly attached, tight root zone was probably effective at blocking the nucleation of quartz

overgrowths; such clay coats, however, do not inhibit the later precipitation of epitaxial cements such as calcite (Cape Roberts Science Team, 2000).

Most authigenic clay minerals studied in sandstones either experimentally or in nature are those found in deeper burial settings common to most petroleum reservoirs. Therefore, the literature has been focused primarily on chlorite, illite, mixed-layer smectite/illite, kaolinite, and dickite rather than smectite (for many examples and case studies, see Scholle & Schluger, 1979, and Houseknecht & Pittman, 1992). In comparison, reports on the occurrence of essentially pure smectite in sandstones in the absence of other authigenic clay minerals are relatively few. For this reason, the occurrence reported here in CRP-3, particularly in the lower portion of the core, may represent a well-defined, well-isolated but less well-documented end member of the diagenetic spectrum.

### CRP-3 SANDSTONES AND CLAY MINERALS

The sequence has been divided into lithofacies associations (Cape Roberts Science Team, 2000). From the top down, the interval from 0.00 to 378.36 mbsf consists of muddy sandstones and mudstones, with subordinate conglomerates and diamictites (Lithofacies Association 5). In contrast, that from 378.36-~580 mbsf was classified as "clean" sandstones (Lithofacies Association 4), whereas Lithofacies Association 3 (~580-789.77 mbsf) has been described as "muddy" sandstones (Cape Roberts Science Team, 2000).

Provenance studies based on both clasts and thin-sections of sandstones detected no alkaline pyroxenes or amphiboles, nor any fresh alkaline-volcanic lithic grains or clasts, and only rare volcanic glass with subalkaline compositions (Pompilio et al., this volume; Sandroni & Talarico, this volume; Smellie, this volume). Hence there are no discernable contributions to the sediment from the McMurdo Volcanic Group of northern Victoria Land. This suggests that McMurdo Group volcanism did not begin in the McMurdo Sound area until *c.* 25 Ma (Cape Roberts Science Team, 2000; also Smellie, 2000 and this volume). Instead, the local TAM provenance seems to have been the source for the CRP-3 sediments, with major inputs from the Beacon Supergroup sandstones and the subalkaline Ferrar Supergroup dolerite sills (Ferrar dolerite), lava flows (Kirkpatrick Basalts), and pyroclastic deposits (Mawson Formation, Kirkpatrick Basalt pyroclasts) (Cape Roberts Science Team, 2000; Neumann & Ehrmann, this volume; Sandroni & Talarico, this volume; and Smellie, this volume).

Chemical analyses for volcanic clasts from CRP-3 are not available. However, Kyle (1998) found that clasts of Ferrar dolerite in CRP-1 are characteristic of those from the TAM, noting that they would be

classified as basaltic andesites using the classification of LaBas et al. (1986). With one exception, silica contents ranged from 53.38 to 56.34 % (Kyle, 1998, Tab. 2).

In thin sections of representative sandstone samples, grain sizes are predominantly fine- to very fine-grained (*c.* 70% of samples; Smellie, this volume). Of significance to the present study, pyroxene grains are an important detrital component (up to 14%). It is fresh and abundant above 180 mbsf, but commonly partially replaced by smectite (or rare carbonate) in samples below that level (Cape Roberts Science Team, 2000). In addition, a variety of lithic grains (up to 9.3% by volume) include dolerite and fine basalt (Smellie, this volume). Volcanic lithic grains reach their highest concentrations below *c.* 600 m (Cape Roberts Science Team, 2000, Fig. 1).

CRP-3 porosity variations indicated by well logs and core measurements do not follow a simple compaction profile such as those usually found in siliciclastic sediment (Hamilton, 1976) and at CRP-1 and CRP-2/2A (Niessen et al., 1998; Brink et al., 2000, respectively). Instead, no systematic depth-dependent porosity decrease is noted below 144 mbsf, apparently due to diagenesis and grain-size fluctuations (Cape Roberts Science Team, 2000, Fig. 2.22). Whereas carbonate cementation augments the compaction profile at CRP-2/2A by reducing porosities in the lower portion of the hole, carbonate cementation at CRP-3 obscures the compaction profile by reducing porosities in the upper part of the hole.

Indeed, carbonate cementation of the sandstones is common, occurring in both greenish "muddy" sandstones and in light-colored clean sandstones (Cape Roberts Science Team, 2000, Fig. 3.12). Carbonate cements and nodules, from 1-43 mm across, were first observed downhole at 234.83 mbsf. These were also present in CRP-2/2A below 500 mbsf (Cape Roberts Science Team, 1999; Aghib et al., 2000). The source of the carbonate in CRP-3 below about 300 mbsf is not clear, as there is "no evidence of the dissolution affecting biogenic tests in terms of incipient/late stage diagenesis" (Cape Roberts Science Team, 2000). Other possible origins might be organic carbon-carbonate diagenesis (Aghib et al., 2000), or hydrothermal fluids that could have passed through Cambrian/Precambrian marbles in the metamorphic basement below the Beacon Supergroup (Cape Roberts Science Team, 2000).

X-ray clay mineral analyses of ethylene-glycolated samples conducted at CSEC made no attempt to determine relative abundances of the various mineral phases (Cape Roberts Science Team, 2000, Tab. 4.5). Chlorites, illites, quartz, plagioclase and a variety of mixed-layer clays occur consistently above *c.* 410 mbsf. Of these, the chlorites and illites are considered to be detrital, produced by physical weathering of Beacon Supergroup and basement rocks

exposed in the TAM. Smectite, 10/17Å mixed-layer clays, and quartz occur consistently below 650 mbsf. Smectite is generally not abundant in modern high-latitude sediments (Griffin et al., 1968; Chamley, 1989) except where volcanic rocks are an important sediment source, even under polar conditions (Ehrmann et al., 1992; Ehrmann, 1998b).

The shift to smectite-bearing assemblages below *c.* 650 has been attributed to one or more of three possible mechanisms to be further evaluated during shore-based studies (Cape Roberts Science Team, 2000): 1) climate then was more humid and possibly warmer, hence greater chemical weathering; 2) sediment sources included volcanic rocks not present during the deposition of younger rocks; 3) diagenesis preferentially produced smectite in the lower part of the section. The latter possibility can best be evaluated by shore-based SEM study (Cape Roberts Science Team, 2000), which is the primary objective of the present study.

## METHODS

Preparations for the SEM were made by fracturing the rock and mounting the fragments on stubs using fast-drying metallic paint. Where sandstones were poorly consolidated, specially constructed, 28-mm-wide dish-shaped holders with raised rims were used to catch any grains that spalled off the sample during examination. Samples were dried in an oven either before or after mounting. Polished sections were examined in the STEM. Examinations in the light microscope were conducted on thin sections (see Smellie, this volume) and smear slides prepared for nanofossil studies (see Watkins et al., this volume).

Porosities, bulk densities, and matrix densities of 82 core-plug samples from CRP-3 and 62 samples from CRP-2/2A were measured by Jarrard (this volume) and Brink & Jarrard (2000), respectively. These data were used to recalibrate the continuous-core and well log data, and to convert the continuous-core density records (Cape Roberts Science Team, 1999, 2000) to porosity (Brink & Jarrard, 2000; Jarrard, this volume). Permeabilities of 50 of these core plugs were measured by TerraTek, Inc. (Salt Lake City, Utah), using a low-pressure (300 psi), continuous-flow, air permeability technique on jacketed samples.

## RESULTS

### AUTHIGENIC SMECTITE CLAY COATS

The overall distribution of smectite, carbonate cement, and mud matrix in CRP-3 noted in thin sections of sandstones is given in table 1. Smectite, occurring as radial rims around grains ("R" in Tab. 1)

Tab. 1 - Down-core distribution of grain size, sorting, cement (carbonate, smectite) and mud matrix in CRP-3 sandstones.

Tab. 1 - Down-core distribution of grain size, sorting, cement (carbonate, smectite) and mud matrix in CRP-3 sandstones

sample	Grain size	Sorting	Cement		Matrix
			Carbonate	Smectite	
3.79	silty VF-F	poor			●
23.32	VF-F (M)	poor			●
67.06	VF-F (M)	poor			●
89.50	silty VF-F (C)	very poor			●
177.22	VF-F	poor-moderate		●	
183.69	VF-F	poor-moderate			○
202.59	F	moderate			●
207.71	VF	well	●	●	
226.42	F-M	well	●	●	○?
235.50	F	moderate			●
240.67	F	moderate	●	●	●
256.66	VF-F	poor-moderate	●	●	●
270.99	M	well	●	●	●
279.68	VF	well	●	●	●
286.17	VF	well	●	●	●
289.22	F-M	moderate-well	●	●	●
315.77	VF-M	poor	○		●
326.67	M	bimodal			●
335.96	VF-F	well	●	●	●
345.76	F-M	moderate			●
348.70	F-M	well	●	●	●
351.88	F-M	well	●	●	●
358.95	F	well	●	●	●
369.64	VF-F	moderate	●	●	●
375.32	F-M	well	●	●	●
383.76	F	moderate-well	●	●	●
387.46	F-M	moderate			●
390.78	F	well	○	●	●
396.58	F-M	well	○	●	●
405.75	silty VF	poor	●	●	●
415.94	VF-F	poor	●	●	●
422.81	F	well	●	●	●
426.77	F	well	●	●	●
437.12	VF	well	●	●	●
445.23	M	well	●	●	●
449.73	F	well	●	●	●
455.81	VF	well	●	●	●
460.15	VF-F	moderate-well	●	●	●
473.61	(F)-M	poor-moderate	○	●	●
475.74	VF	well	○	●	●
480.68	F-M	moderate	●	●	●
481.72	F-M	poor-moderate	○	●	●
486.05	F	well	○	●	●
495.15	F-M	moderate-well	○	●	●
500.71	F-M	moderate-well	○	●	●
509.36	F	well	●	●	●
513.17	(F)-M	moderate	●	●	●
535.76	M	moderate	●	●	●
533.76	M-L	poor-moderate	●	●	●
543.87	VF-F	poor	○	●	●
550.05	VF-F	poor	○	●	●
571.80	F	well	○	●	●
615.37	VF-F	well	○	●	●
676.18	(VF)-F	poor-moderate	●	●	●
630.38	F	moderate	●	●	●
643.11	F-M	poor	○	●	●
655.86	VF	moderate-well	●	●	●
664.05	F	well	○	●	●
673.78	VF-F	moderate-well	●	●	●
681.02	VF-F	moderate-well	●	●	●
686.52	F	well	○	●	●
696.77	VF-F	moderate-well	●	●	●
715.48	F-M	poor-moderate	○	●	●
724.08	VF-F	well	○	●	●
730.87	VF	moderate-well	●	●	●
735.39	VF	well	○	●	●
737.35	VF-F	moderate	●	●	●
750.02	VF	poor-moderate	○	●	●
770.26	VF-F	poor-moderate	○	●	●
787.66	VF	poor-moderate	○	●	●

● Pervasive, abundant	R Radial authigenic smectite
● Patchy, minor	L Laminated allogenic smectite
○ Trace	thick Thick authigenic smectite (>5 microns)

and therefore presumed to be authigenic, is not only present, but pervasive and abundant from Samples 335.96 (mbsf) to 787.66; those from Samples 630.38 to 737.35 and one at 770.26 mbsf are distinguished as “thick”, *i.e.* greater than 5 micrometers. The presence of such clay coats in Sample 389.32 from the upper third of the hole is confirmed by STEM images of polished sections in figures 3a-c, where the coats are of reasonably uniform thickness and surround the grains nearly completely except where they are pressed most closely against one another (arrows). In figures 3a and 3c, the interstices are filled by calcite cement that postdates the clay coats.

A scanning electron micrograph of a fracture surface through a silty sandstone at 706.58 mbsf displays an assortment of grain sizes ranging from 10 to over 400 microns (Fig. 4a). These sands were sourced from Beacon Supergroup strata, primarily the Triassic volcanogenic Lashly Formation (Smellie, this volume). The individual sand grains are uniformly

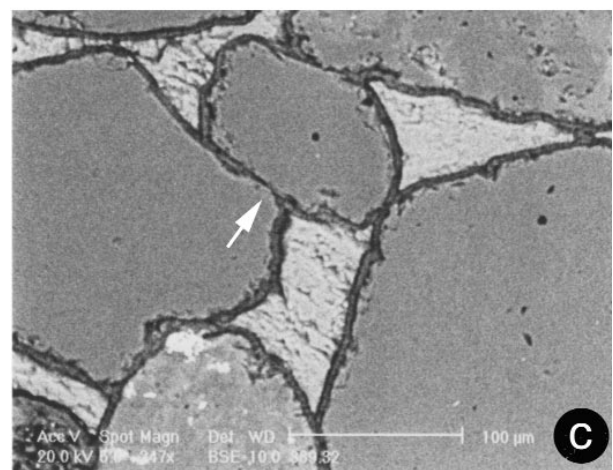
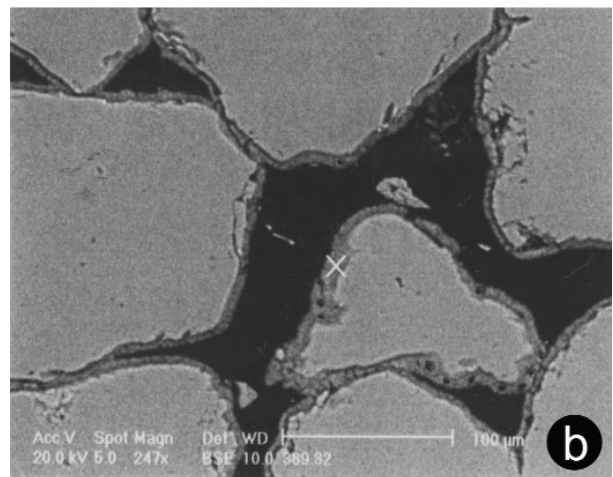
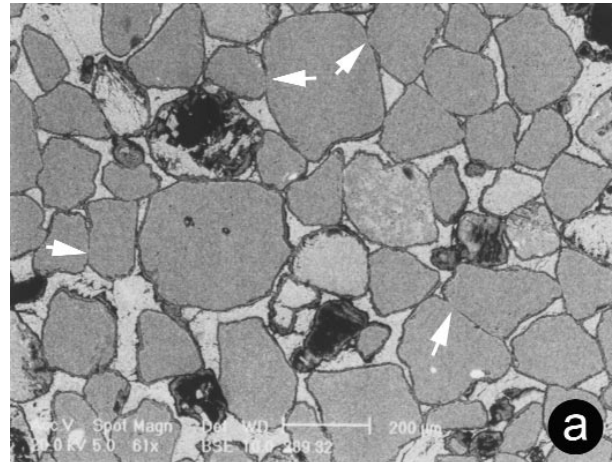


Fig. 3 - a) STEM micrograph of a polished section of a CRP-3 sandstone from 389.32 mbsf showing primarily quartz grains coated by authigenic smectite and cemented by a late-stage calcite. Arrows point to some of the few places where the smectite coats are thinned or missing due to compaction of the sand grains. Bar scale = 200 microns. b) Same specimen as above in an area of the sample not cemented by calcite. Bar scale = 100 microns. c) Same specimen as above in an area cemented by calcite. Arrow points to one of the few places where the smectite coats are thinned or missing due to compaction of the sand grains. Bar scale = 200 microns.

coated with smectite. In many places, however, patches of the coats were torn away when the sample was fractured (Figs. 4b and 4c), revealing the smooth surfaces of the quartz grains beneath (“Q” in Fig. 4c; see labeled boxes in Fig. 4b for the location of this figure as well as Figs. 4d and 4e).

In plan view, the clay coats display the dense polygonal box-work pattern of individual platelets that

is characteristic of well-developed authigenic smectite (Fig. 4d; compare with Wise & Ausburn, 1980, figs. 8-10; Pittman et al., 1992, figs. 20C-D). In contrast, somewhat smoother “bald spots” represent grain-contact scars (“S” in Fig. 4c), *i.e.* points of contact where sand grains were pulled away when the sample was fractured (see Hathon & Houseknecht, 1992, fig. 6D caption). These expose the dense root zone at the

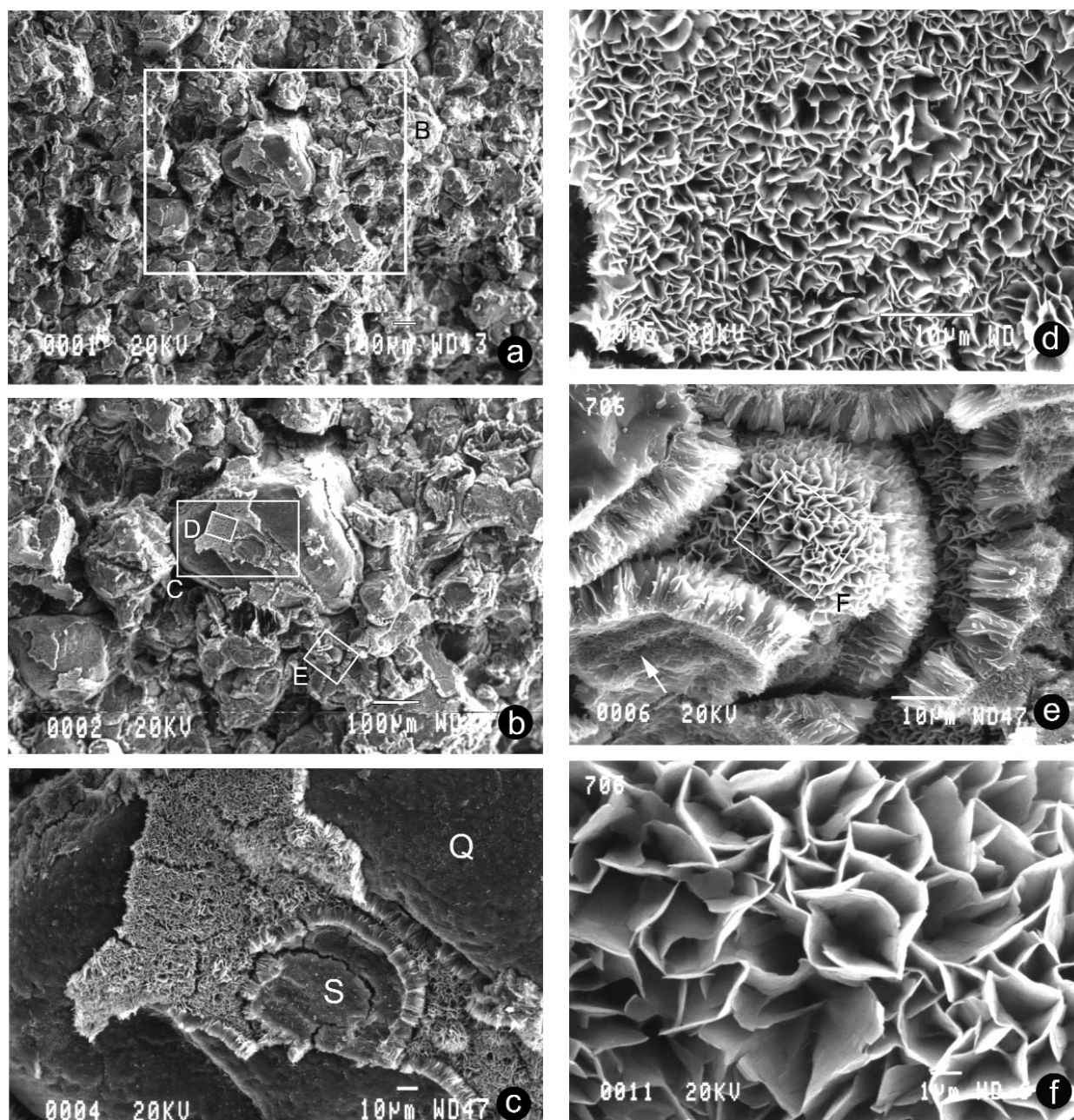


Fig. 4 - a) SEM of a fracture section through a CRP-3 sandstone sample from 706.58 mbsf; area outlined by white rectangle enlarged in figure 4b below. Bar scale = 100 microns. b) Enlargement of figure 4a showing large sand grain with part of its smectite coat torn off when the sample was fractured. White boxes show locations of figures 4c, d, and f. Bar scale = 100 microns. c) Enlargement from figure 4b showing where part of a smectite coat was removed during sample preparation to reveal the smooth surface of a quartz sand grain beneath (“Q”). A “bald spot” or grain-contact scar “S” in the center of the figure also exhibits a smooth surface. Fractures in the clay coats are probably artifacts of sample preparation. Bar scale = 10 microns. d) Enlargement from figure 4b showing in plan view the characteristic honey-comb or box-work pattern of smectite platelets comprising a clay coat. Bar scale = 10 microns. e) Enlargement of figure 4b showing radial growth of smectite platelets into an interstice of the sandstone. Arrow points to a “bald spot” or grain-contact scar on the underside of a clay coat. Bar scale = 10 microns. f) Enlargement of figure 4e above showing euhedral nature of the smectite platelets. Bar scale = 1 micron.

base of the clay coats. Fracturing may have also produced the cracks seen in the clay coats of figure 4c.

The free growth of the smectite platelets within the interstices of the sandstone is illustrated in figure 4e. The idiomorphic nature of the individual platelets is shown in close-up view in figure 4f. Cross sections of the clay coats in figure 4e demonstrate the radial nature of their growth; these coats measure up to 10 microns in thickness. This fractograph also reveals a "bald spot" (arrow) on the underside of one of the coats, where the grain that formed the substrate was removed when the sample was fractured.

The relationships among the clay coats noted above have also been observed in a coarser-grained sandstone from 716.44 msbf (Fig. 5). Again the thickness of the dense authigenic clay coats is quite uniform. Missing patches of clay coats are artifacts of fracturing during sample preparation. In this sample small crystals of an unidentified substance (zeolite, calcite, or quartz?) form a late-stage precipitant on the clay coats (Fig. 5c).

#### POROSITY AND PERMEABILITY

Measured intergranular permeabilities of the CRP-3 and CRP-2 samples encompass a range of more than five orders of magnitude. Intergranular permeabilities of most sedimentary rocks are controlled by pore geometry, which in turn is dependent on porosity and lithology. This dependence often results in a linear relationship between porosity and the logarithm of permeability for all rocks from the same formation (Nelson, 1994).

The relationship between porosity and permeability for five intervals of CRP-2 and CRP-3 is shown in figure 6. These intervals have generally similar porosity ranges, but distinctively different permeabilities for a given porosity. All CRP-2/2A samples, as well as the top 200 m of CRP-3, define a single permeability/porosity trend that is much lower in permeability than deeper CRP-3 samples, despite generally higher porosities. This trend, which is similar to those found in some shales but much lower than those of published sandstones (*e.g.* Nelson, 1994), indicates a poorly connected pore geometry that may be attributable to the muddiness of most of these sediments. Though these two intervals come from different wells, they are stratigraphically adjacent portions of the ~1700 m composite CRP-1/2/3 section (Cape Roberts Science Team, 2000, Fig. 7.9), with identical permeability/porosity relationships and with generally similar lithologies (muddy sandstones, siltstones, and diamicts).

CRP-3 samples from 370-766 mbsf have a permeability/porosity relationship characterized by much higher permeabilities and much greater sensitivity of permeability to porosity than that from CRP-2 and uppermost CRP-3 (Fig. 6). The

permeability/porosity pattern for this deeper interval is similar to that of sandstones from many parts of the world (Nelson, 1994). Samples from the intervening section (223-361 mbsf) appear to define an intermediate permeability/porosity relationship (Fig. 6), but it is also possible that they represent a transition zone of alternating beds of deeper and shallower permeability/porosity behavior. Although

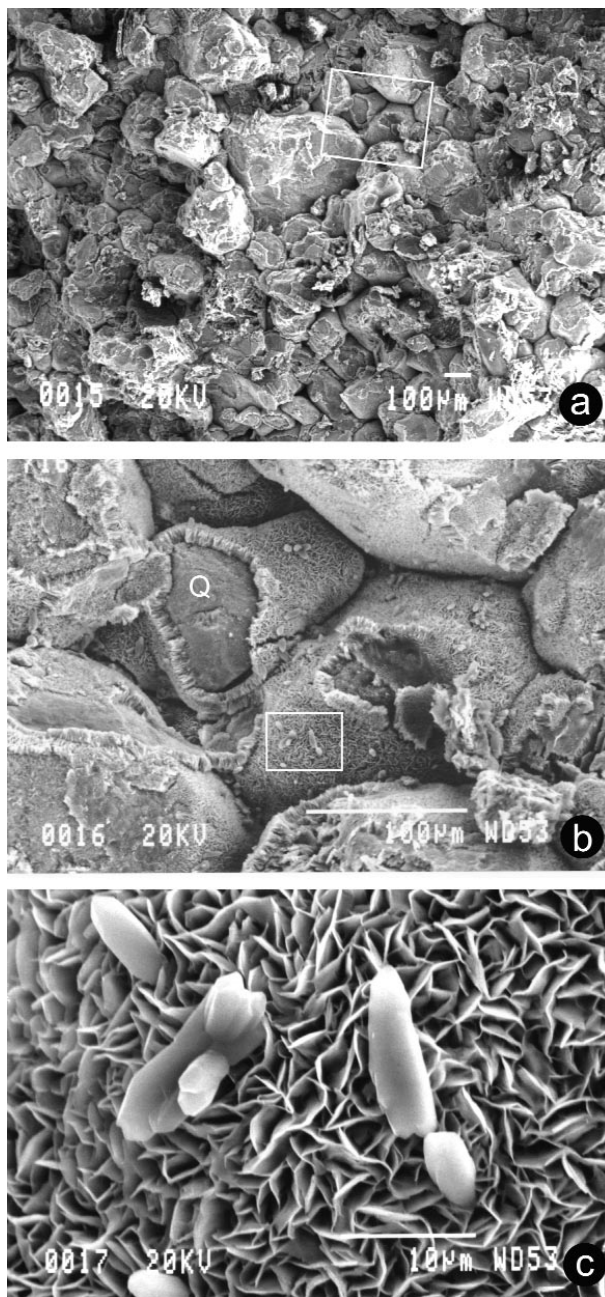


Fig. 5 - a) SEM of a fracture section through a CRP-3 sandstone sample from 716.44 mbsf showing area (white box) enlarged in figure 5b below. Bar scale = 100 microns. b) Enlargement of figure 5b above, showing smectite coats, parts of which were torn off when the sample was fractured, exposing the smooth surface of the quartz grain ("Q"). White box shows location of figure 5c below. Bar scale = 100 microns. c) Enlargement of figure 5b above showing dense pattern of the smectite platelets on which some unidentified (zeolite, calcite, or quartz?) crystals have been precipitated. Bar scale = 10 microns.

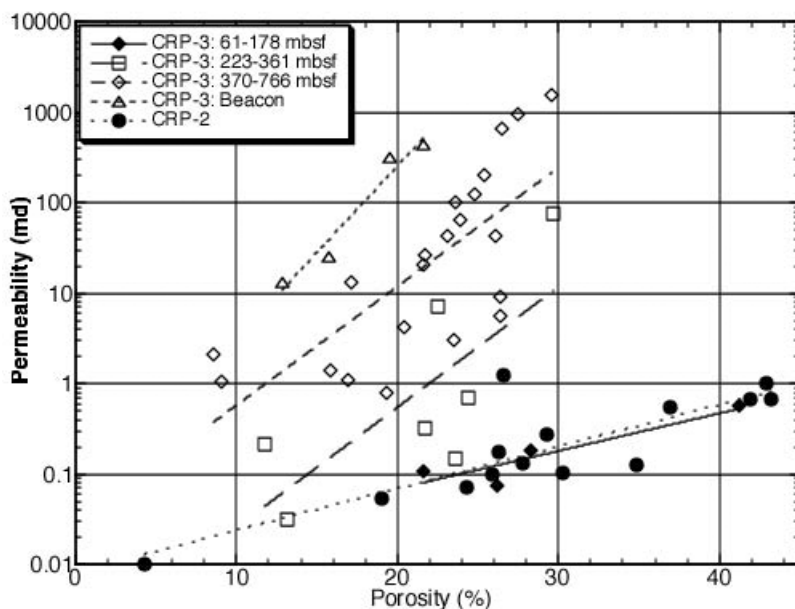


Fig. 6 - Permeability/porosity trends based on core plug measurements for five intervals in CRP-2 and CRP-3. The trends in the lowest Cenozoic section of CRP-3 (370-766 mbsf) and the Devonian Beacon Supergroup sandstones are much higher in permeability than in the overlying Cenozoic of CRP-3 and CRP-2.

only four samples of Devonian Beacon Sandstone were measured, their pattern is apparently significantly different from the deep Tertiary (370-766 mbsf) results, with permeabilities that are an order of magnitude higher for a given porosity. This permeability enhancement is compatible with the suggestion of Jarrard (this volume) that the Beacon has a more open and continuous pore geometry than Tertiary sediments at CRP-3, based on comparison of plug formation-factor vs. porosity relations.

The relationships between permeability and porosity in figure 6 can be used to predict permeabilities where only porosity data are available. Assuming that the short CRP-1 section has a permeability/porosity relationship similar to the one for all of CRP-2 and upper CRP-3, and that the CRP-3 intervals 200-365 mbsf, 365-823 mbsf, and 823-939 mbsf have distinctively different relationships as shown in figure 6, one can convert all continuous-core porosities for the composite CRP-1/2/3 stratigraphic section to permeability. Individual predicted permeabilities may be inaccurate by as much as an order of magnitude, based on observed dispersion in figure 6, but zonal permeability patterns indicated by hundreds to thousands of measurements should be reasonably representative. It should be noted, however, that no core-plug sampling was undertaken in the many thin conglomerates, and the clast-induced low porosities and consequently low predicted permeabilities of these beds may be biased.

Permeabilities for the composite CRP-1/2/3 section as a function of depth are plotted in figure 7. To facilitate comparison to discussions of CRP-3 depth in this paper, we use current CRP-3 depths (in mbsf) as the reference frame for this figure (*i.e.* top of CRP-3 = 0 mbsf; CRP-2 and CRP-1 sections stacked above are measured from that point upwards in negative numbers). The core-plug measurements (open circles,

Fig. 7) clearly demonstrate a pattern of systematically higher permeabilities below about 200-400 mbsf than in uppermost CRP-3 and all of CRP-2 and CRP-1. However, permeability variations of as much as two orders of magnitude between adjacent samples obscure the detailed character of this transition.

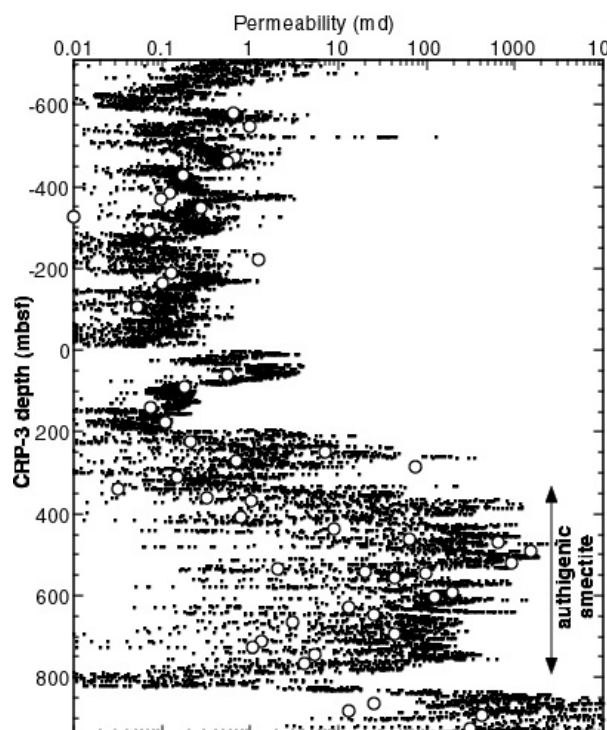


Fig. 7 - Permeability profile based on core-plug measurements (open circles) and porosity-based predicted permeabilities (continuous tracing) for the composite CRP-1/2/3 section as a function of depth using the current CRP-3 depths (in mbsf) as a reference frame (*i.e.* top of CRP-3 = 0 mbsf; sections stacked above are measured from that point in negative numbers). Permeabilities are systematically higher below about 200-400 mbsf, which corresponds to the zone of authigenic smectite precipitation (arrow).

Porosity-based predicted permeabilities (Fig. 7, continuous tracing) provide a more detailed permeability structure for CRP-1/2/3. However, predicted permeability variability within the ~200-365 mbsf transition zone may be underestimated because of our use of a single, average permeability/porosity relationship for this interval.

The interval from approximately 350 to 790 mbsf has permeabilities that are consistently two orders of magnitude higher than in bracketing zones. This interval closely corresponds with that previously described as the authigenic-smectite interval (Fig. 7, vertical arrow). The base of this high-permeability interval is sharp, at the 789 mbsf boundary between overlying sandstones and underlying doleritic breccia. Plug permeability measurements were impossible within this doleritic breccia, so its permeability/porosity relationship is unconstrained. Actual intergranular permeabilities within this doleritic breccia are probably even lower than the very low values predicted in figure 7, because the breccia matrix is predominantly clay (Cape Roberts Science Team, 2000).

The relevance of the present CRP permeability structure of figure 7 to CRP diagenesis depends on two critical assumptions. First, intergranular permeabilities such as those shown here affect intergranular flow. The overall flow pattern can be dominated by localized flow in faults or fractured intervals, because fracture permeability is commonly orders of magnitude higher than intergranular permeability. Indications of fracture permeability variations within CRP-3 are discussed in a later section. Second, the palaeoflow responsible for diagenetic precipitation of smectite and calcite responded to palaeopermeability, not present permeability. For these high-porosity sandstones, authigenic smectite or calcite probably reduces permeability mostly by reducing porosity. A 5-10% porosity reduction within CRP-2 and uppermost CRP-3 attributable to calcite precipitation is expected to reduce permeability by ~50%, comparable to the effect of ~2% porosity reduction in lower CRP-3 due to authigenic smectite. Both temporal changes are minor compared to the two orders of magnitude permeability difference between these zones.

## DISCUSSION

### AUTHIGENIC CLAY COATS

Many questions have arisen during the course of this investigation regarding the source, timing and mode of emplacement of the smectite clay coats described above, not all of which can be answered at the present time. The results given above, however, do show that the smectite coats, especially those in the lower portion of the core, are clearly authigenic, having precipitated from solution as evidenced by: 1)

their radial growth habit and, in plan view, polygonal box-work structure (*e.g.* Fig. 4d) as well as 2) well-formed, large euhedral platelets (*e.g.* Fig. 4f). In addition they exhibit a well-crystallized structure and a near monomineralic composition.

The high degree of crystallization has been demonstrated by complementary geochemical and mineralogical studies carried out by Ehrmann and Setti et al. (both this volume). These authors report that the clay fraction below 602.05 mbsf is not only made up almost exclusively of smectite (see x-ray diffractograms by Setti et al, Fig. 1 and Ehrmann, Fig. 3), but yields the highest values on their crystallinity indices (from Biscaye, 1965; Thorez, 1976; *cf.* Ehrmann, 2000; *cf.* Diekmann et al., 1996). Setti et al. find that these smectites are Mg-rich, and fall within the intermediate beidellite-saponite distribution field. This is in contrast to those in the upper 100 m of CRP-3, where the smectites have a slightly lower crystallinity index and are considered detrital in origin. In the central part of the core between 154.45 and 522.73 mbsf, these authors find a high degree of chemical variability indicating some degree of mixing of detrital clays (see also Ehrmann, this volume).

The interval from ~580 to 789.77 mbsf in CRP-3 was initially described as a "muddy" sandstone (Cape Roberts Science Team, 2000). Shore-based observations confirm that the "mud" in this interval is mostly authigenic smectite, not a detrital clay, although there are several intervals of muddy horizons or zones that may contain such minerals (*e.g.* 757.44 to 764.68 mbsf). Most of the quartz-dominated sandstones, therefore, were originally quite clean upon deposition. Indeed, textural analysis shows that with the clay fraction excluded, this part of the core is almost entirely sand from a very near shore (sometimes beach?) environment (Barrett, this volume). The environment, however, was quite likely marine, as no authigenic corrensite has been detected.

It is clear from both light microscopy and electron micrographs that the smectite coats consist of only a single layer, which represents a single generation of cement emplacement. The exact time of this emplacement cannot be determined from the current data. For now, we can only speculate on the relative time of emplacement based on the stratigraphic occurrence of the clay coats, the presence of other cements, and the burial history as we understand it.

Unfortunately, the age of the sediments in which the authigenic smectites occur (those below *c.* 350 m) is poorly dated as early Oligocene to possibly Eocene. The base of the Cenozoic sequence is probably very close to the Eocene/Oligocene boundary. These sediments lie below the last downhole occurrences of calcareous nannofossils and diatoms, the groups that have proven most useful in dating the upper portion of the core. These

microfossils date the top 200 m of the core as being younger than *c.* 33 Ma (Chron C13n) (see Harwood & Bohaty, Watkins et al., both this volume). Whether or not the Eocene was reached by the core is a subject of considerable debate and speculation (compare Ehrmann, Florindo et al., Harwood & Bohaty, Hannah et al., Thorn, and Sagnotti et al., all this volume). We only know for certain, therefore, that the smectite was emplaced in sandstones at least 33 million years old. Its precipitation, however, could have occurred at any time after the deposition of those sediments. We can also say that the smectite cement formed before the development of the carbonate cements and nodules. However, we as yet have no other data on the time of this carbonate precipitation.

Spötl et al. (1994) list three textural criteria that point to early precipitation of chlorite in a Pennsylvanian reservoir sandstone they studied from Oklahoma: 1) high intergranular (pore-space) volumes of the host sediment, 2) thinned coatings between contacts of framework grains, and 3) the fact that all other diagenetic phases appear to postdate the clay precipitation. Our example from CRP-3 meets all three of these criteria. The coatings cover all of the framework grains rather uniformly, except at the relatively few places they have been closely appressed during compaction (arrows, Fig. 3a). This indicates that the grains were little compacted when the coats formed, thereby allowing the precipitating fluid access to most of the grain surfaces. Subsequent compaction has done little to thin the original coats. These grain relationships are frozen in place where the rocks have been cemented by calcite. At 389.82 mbsf there is little noticeable difference in compaction between the carbonate-cemented and carbonate-free samples (Fig. 3). Thus at these depths, little compaction seems to have taken place since the calcite cementation. In other words, the sediment had reached its maximum burial depth when this cementation occurred.

#### SOURCES FOR SMECTITE PRECIPITATION

To precipitate authigenic smectite from pore-fluid solutions, one must have a source of silica and cations plus the necessary physicochemical conditions (temperature, pressure) plus time for the reaction to proceed. Volcanic materials are an ideal source, particularly in cold-climate conditions as existed here, where chemical weathering is minimal. These could be present within the Cenozoic sediments themselves or as intrusions within the “basement” rocks beneath or adjacent to the rift basin.

As discussed previously, volcanic materials derived from the Ferrar Supergroup, occur as clasts and finer particles within CRP-3, particularly in the lower 200 m of the Cenozoic section. Many of the volcanic clasts and detrital pyroxenes have been altered to smectite (Cape Roberts Team, 2000; Pompilio et al.,

this volume; Smellie, this volume). In addition, a highly altered sill was encountered within the Devonian sandstone beneath (Unit. 17.1). Field occurrences of altered Ferrar dolerites in the Transantarctic Mountains are unknown (Kyle, 1998), therefore either burial diagenesis or hydrothermal waters was likely responsible in this case. Hydrothermal fluids might be associated with Cenozoic faulting along the margin of the rift basin (Fig. 2; Cape Roberts Team, 2000, Figs. 7.7 and 7.8). In either case, there seems to be sufficient intraformational volcanic material within the sedimentary column to provide a source of cations for smectite formation.

As to a supply of silica, the alteration of volcanic materials mentioned above would be the most likely source. It should be borne in mind, however, that the supply of volcanic materials in this quartz-dominated sequence is considerably less than in many of the examples cited in the ‘Previous Work’ section, such as the Woodbine Sandstone or the Quaternary volcanic sands of Guatemala. Nor would the basalt and dolerite of the Ferrar Supergroup be as silica-rich as those examples mentioned above or for the Tuscaloosa Fm, the andesitic Mehrten Formation of California, and the rhyolitic precursors for the Great Plains sequence, Ponza and Kinny bentonites.

Diatoms would have been one likely and convenient source of silica although their presence may have been scanty judging from their abundance in lower Oligocene strata at the CIROS-1 drill site some 60 km south of CRP-3. The fact that they were preserved in sediments of equivalent age or older down to 700 mbsf in the CIROS-1 core (Cape Roberts Team, 2000, Fig. 5.3), however, suggests that their total absence in the lower part of CRP-3 is due to diagenesis. Even where preserved at the top 200 m of CRP-3, their preservation diminishes markedly below 67 mbsf.

This generalization is contradicted only by the presence of phytoliths, a more robust form of amorphous silica, in the lower portions of the core (Thorn, this volume), and trace amounts of fresh brown, green and colourless glass of subalkaline composition (believed derived from Jurassic Kirkpatrick Basalt; Pompilio et al., this volume) that were not dissolved (see discussion below).

#### SMECTITE EMPLACEMENT

As to the mechanism of smectite emplacement, we explore below three possibilities.

##### **A case for smectite precipitation during burial diagenesis**

A case for smectite authigenesis as a result of burial depends on 1) identifying an adequate source of precursor material within the sedimentary sequence and 2) on demonstrating that the necessary heat/temperature/time conditions were attained that

would allow *in situ* diagenesis to proceed. These two factors are examined below.

#### *Correlation of Smectite Occurrence and Basic Intraformational Sedimentary Components*

As indicated in table 1, the authigenic smectite coats are present rather consistently from the lowermost Cenozoic marine sandstone sampled at 787.66 mbsf up to 335 mbsf, and this might suggest that they precipitated from a uniformly distributed and well-circulated pore-water medium that affected this stratigraphic interval.

On the other hand, minor gaps in the occurrence of the smectite clay coats extend from 486.03 to 525.36 and 445.23 to 449.47 mbsf, and they are patchy in Samples 455.81 to 475.34 mbsf (Tab. 1). The thickest coats occur in the lower 137 m of the sequence. In comparing the data, a visual inspection with that in table 1 and the CRP-3 *Initial Reports* (2000, Tabs. 4.6, 4.8 and Figs. 4.1 and 4.8) suggests the following:

Ferrar dolerite clasts and pyroxene grains (dolerite-derived) are least abundant from 410 to 530 mbsf, which encompasses the intervals with few or no smectite coats mentioned above. Conversely, dolerite clasts, volcanic lithic and pyroxene grains are

particularly common below 660 mbsf, where the coats are thickest. If the proportion of these detrital components can be taken as a rough indication of the amount of fine volcanic detritus in the core, then the primary source for the smectite coats was dispersed within the Cenozoic sediments. These correlations are far from exact, however, and our ad hoc assumption that those detrital constituents accurately reflect the distribution of finer volcanic materials is unproven but strongly permissive.

To further test these correlations, we have replotted the smectite occurrences given in table 1 against the grain counts (in thin section) given in tables 4.6 and 4.8 as supplemented by more recent shore-based data (Smellie, unpublished). These correlations are shown in figure 8, where a smectite abundance curve is fitted visually over the actual occurrences, whereas pyroxene grains are expressed as percent and by a curve derived statistically (based on 50-m running means). The basaltic lithic volcanic grains are also expressed as 50-m running means, and include grains of likely Kirkpatrick basalt, basic lavas (source undetermined, probably a mixture of Kirkpatrick and Ferrar dolerites), and graphic-textured grains likely derived from Ferrar dolerites.

There is an apparent correlation between the

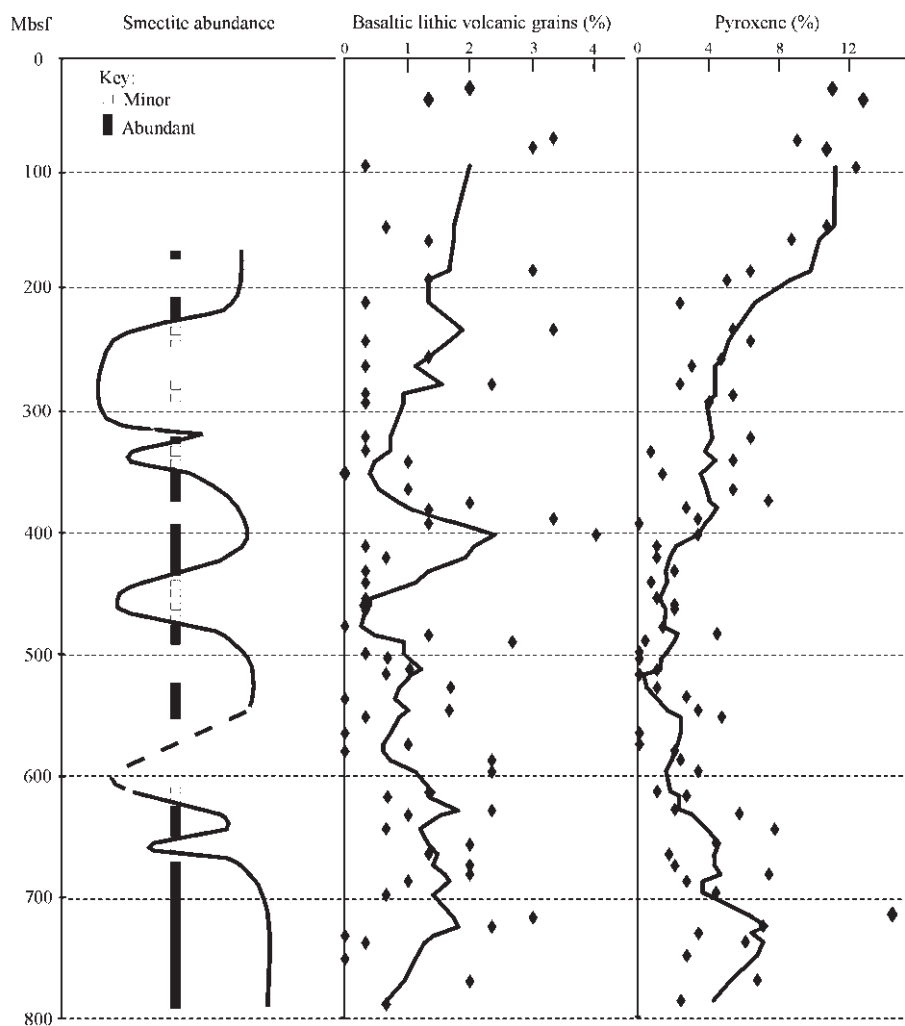


Fig. 8 - Comparison of smectite abundance, percent basic volcanic grains and percent pyroxene grains with depth in CRP-3. Smectite curve shown is a visual depiction based on petrographic abundance. Other curves are statistically derived, based on 50 m running means. Despite the large data scatter for basic lithic volcanic grains, there is a strong correspondence with peaks and troughs for smectite abundance, whereas there is no obvious correspondence between smectite and pyroxene abundances.

basaltic lithic volcanic grain abundance and authigenic smectite occurrence, but none between pyroxene grain abundance and authigenic smectite, except for a very weak correspondence below 600 mbsf (Fig. 8). We believe that the correlations depicted in figure 8 demonstrate that the intraformational basaltic lithic volcanic grains represent a highly likely source for the authigenic smectite, although we leave open the possibility of additional contributions from the dolerite breccias and conglomerates immediately below.

#### Burial History vs Smectite Authigenesis

A subsidence curve for the Cape Roberts area was calculated based on a composite of age and depth data for all three CRP sites plotted from the position of CRP-1 (Fig. 9). In essence, the three drill holes were stacked stratigraphically, taking into account a slight overlap between CRP-1 and -2, and a slight gap between CRP-2 and -3 (Cape Roberts Science Team, 2000, Fig. 7.9). No account was taken for compaction, the many unconformities detected in the section, or the tendency for the sections to thicken to the east as shown by the seismic reflection reconstruction in figure 1. Nevertheless, this curve is taken as a reasonable approximation for the minimum burial depth experienced by the oldest Cenozoic sediment at site CRP-3. Because a major unconformity represents most of the early Quaternary to Miocene interval (between about 1 and 17 Ma) at all sites, the depths shown are taken as a minimum, bearing in mind, however, that unconformities could indicate non-deposition as well as erosion of preexisting sediments.

Based on the age dates currently available, sedimentation rates during the early Oligocene were extraordinarily high, as much as 200 m/m.y.; however, concurrent rifting that created the Victoria Land Basin was such that the site of deposition remained at shelf depths, close to or sometimes above storm wave base (Cape Roberts Science Team, 2000, Fig. 7.4). Eventually both subsidence and sedimentation slowed somewhat as the basin appeared to shallow (above 580 mbsf in CRP-3; Fig. 2) and the marine sands became cleaner and better sorted. A glacial influence is indicated by sparse drop stones. At 380 mbsf, however, clean sands become rare and are replaced by muddy sands, muds, diamictites and conglomerates as subsidence outpaced sedimentation in a glacio-marine, open-shelf environment subject to many cyclical glacial advances and retreats.

Considering the relatively basic chemical composition of the volcanic materials and the scarcity of biogenic precursor materials at CRP-3, one would not expect smectite authigenesis to proceed as readily in these sandstones as in many of the more siliceous examples cited in the 'Previous Work' section. Temperatures and pressures above near-surface conditions would probably be necessary to cause the dissolution–diffusion–reprecipitation reaction necessary

to form the thick smectite coats within the relatively clean sandstones in the lower portion of the hole.

Taking into account age/depth considerations, the window for authigenic smectite formation, however, would certainly have been reached by the time the site passed beneath 800 mbsf, at about 30 Ma (Fig. 9). The present-day average geothermal gradient at CRP-3 is about 28.5° C/km based on downhole logging, which measured a near bottom-hole temperature of 23° C at 870 mbsf and a seafloor temperature of -1.8° C (Cape Roberts Science Team, 2000; Bücker et al., this volume). The gradient is somewhat less than the 35° C measured at CIROS-1, where diatom frustules were preserved throughout the hole. Based on the present-day gradient, temperatures at 800 mbsf (near the bottom of the Oligocene marine sequence) would have been 22° C at about 30 Ma and 40° C at 17 Ma, at which point a depth of 1400 mbsf was reached (Fig. 9). Temperatures at the highest stratigraphic occurrence of authigenic smectites in CRP-3 (336 mbsf) at these times would have been about 16° C and 30° C respectively.

These temperature estimates must be considered minimum values because temperatures must have been higher when rifting was most active (Moraes & De Ros, 1992 citing Daniel et al., 1989, and McKenzie, 1978), *i.e.* during the Oligocene. Furthermore, there may have been an influence of warm circulating fluids (see Cases 2 and 3 below), although very rapid fluid flow would be necessary to raise ambient temperatures significantly.

The absence of these clay minerals above 336

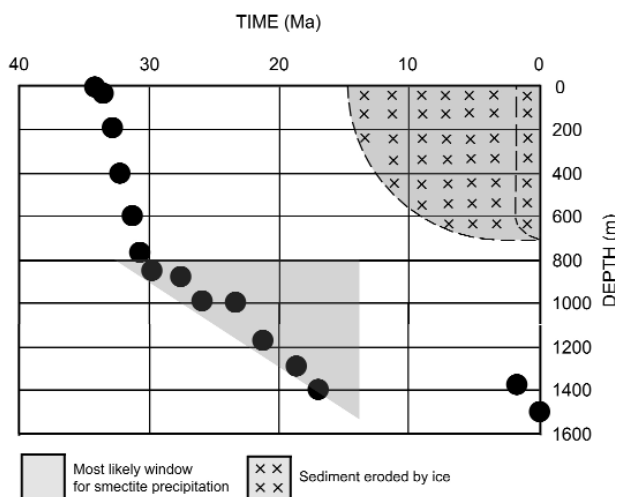


Fig. 9 - Subsidence curve for the floor of the Victoria Land Basin at the location of CRP-1 through time, projected by stacking stratigraphic sections from CRP-2/2A and CRP-3 to the CRP-1 site (after Cape Roberts Science Team, 2000, fig. 7.6). No corrections have been made for compaction, unconformities, or faults within the section. The figure shows rapid subsidence from 34 to 31 Ma, followed by slower subsidence to 17 Ma, with essentially no net subsidence from then to the present day. The "xxx" pattern indicates the amount of section believed to have been eroded from the top of CRP-3 by Neogene glacial erosion beginning either about 15 Ma or 2.5 Ma. The shaded pattern represents the optimal window for precipitation of authigenic smectite from thermobaric waters at Site CRP-3.

mbsf sets an upper limit on the conditions necessary for smectite precipitation if temperature and pressure were the primary controlling factors. It has been argued, however, that “temperature effects have been overemphasized in evaluating many diagenetic reactions associated with burial” (Surdam & Boles, 1979). In the present case, the loss of permeability at about this level (Fig. 7), therefore, was probably a more important controlling factor as this would have inhibited the free diffusion of ions or the possible circulation of fluids from below.

In any event, it appears, based on comparisons with other examples at similar burial depths (*i.e.* the Tuscaloosa Fm, Pittman et al., 1992), that burial diagenesis alone could have generated the smectite coats in CRP-3. Some questions remain to be answered, however.

For instance, we are puzzled that opal-A phytoliths and persistent though rare traces of volcanic glass observed in smear slides would have survived in the same setting in which the smectite precipitated, assuming that the clay was sourced from that same unit. We do note, however, that diagenesis within source units is not necessarily even. Lerbekmo (1957, p. 31) reported that many lithic volcanic fragments as well as scattered glass shards remained unaltered in the Mehrten Sandstone of California, whereas others had clearly been converted to smectite.

Regardless of whether burial diagenesis alone was responsible for the smectite in CRP-3, it is evident that the temperatures involved were never elevated much above 60° C, otherwise illite and perhaps quartz would have been expected to form. This is borne out by the condition of organic-walled dinoflagellates and acritarchs, which retained their natural color, even at the bottom of the Cenozoic section (J. Wren, pers. comm., 2001). This indicates that they did not enter the oil-generating window, which begins at about 75° C.

In addition, oxygen-isotope analyses of the carbonate cements suggest a low-temperature environment. Although the  $\delta^{18}\text{O}$  values are quite negative (-7 to -10‰ at 32.39 mbsf and *c.* -18 to -21‰ at 787.84 mbsf), they are attributed to meteoric waters entering the formation from melting glaciers (F. Aghib, personal communication). We agree with this interpretation because if these negative values were attributed to elevated temperatures, then the bottom of the Cenozoic section would have been at 150-200° C (Craig, 1965; O’Niel et al., 1969), which is not compatible with the available clay mineral and palynology data.

It should be noted that pervasive meteoric-water flushing of subcrop formations may promote the leaching of more soluble minerals such as feldspar, thereby generating early diagenetic clays such as kaolinite in warmer climes (Bjørlykke & Aagaard, 1992). We have not yet tried to assess the possible role of such waters at CRP-3.

Based on the present-day sediment bathymetry at

the Cape Roberts sites (Fig. 2) and the known glacial history of the region, one may assume removal of the post-lower Oligocene sediments at CRP-3 by intense glacial erosion, probably after the formation of a permanent “polar” (dry-based, cold and stable) East Antarctic Ice Sheet, beginning at about 15 Ma or as late as 2.5 Ma, depending on which model of ice-sheet history one wishes to follow (e.g., see Stroeven et al, 1998 vs Harwood & Webb, 1998, respectively, as summarized by Miller & Mabin, 1998). Such erosion planed the Cenozoic marine section at CRP-3 down to its present thickness of about 800 m. This excavation of the sediment above site CRP-3 is indicated on figure 9. The time that this erosion occurred is important because removal of the sediment above the site probably reduced the overburden by half, thereby removing the site from the realm in which the authigenic smectite would most likely have formed.

#### Summary

Considering the strong correlation between the occurrence of the radial smectite coats and intraformational precursor materials in addition to a burial history conducive to smectite authigenesis, we believe a reasonably strong case can be made for *in situ* diagenesis as the origin of the authigenic smectite. The probable window for its formation of the authigenic smectite was between 30 Ma and 15-2.5 Ma. No matter which time estimate is taken for the truncation of the section by glacial erosion, there was ample time (15 m.y. or more) for smectite precipitation to occur within this window, considering how fast authigenesis can proceed (Gluyas & Oxtoby, 1995). We speculate that the erosion that removed much of the overlying section, however, probably precludes the possibility of smectite formation at the site today.

#### A case for smectite precipitation from hydrothermal waters

Establishing a case for smectite precipitation based on age/depth considerations does not at this time preclude the possibility of emplacement by other mechanisms. The interpreted seismic reflection section shows that CRP-3 overlies an upthrown, tilted basement block bounded by a graben to the west (Cape Roberts Team, 2000, Figs. 7.7 and 7.8).

Microfaults are abundant throughout the CRP-3 core and “record significant strain, suggesting the proximity of one or more major faults” (Cape Roberts Science Team, 2000, p. 200). Brittle fault zones evident in the core at 257-263 and 539 mbsf (Fig. 2) are characterized by calcite veining and by high-fracture permeabilities, based on both loss of drill fluids into the borehole and temperature anomalies measured after drilling (Cape Roberts Science Team, 2000). Additional temperature anomalies indicative of drilling-induced flow into zones of high fracture

permeability occurred at 606, 748, and 840 mbsf (Cape Roberts Science Team, 2000; Bücker et al., this volume); the deepest of these corresponds with the highest core-based fracture abundance of the entire hole. All except the 539-mbsf fault zone exhibit high log-determined porosities. In contrast, a third inferred shear zone between 790 and 806 mbsf (Fig. 1) includes cataclastic features, glassy smectite-rich matrix, low porosities, and little or no temperature anomaly indicative of fracture permeability. Both the Beacon strata and the dolerite intrusion are characterized by extensive faulting and brecciation (Cape Roberts Team, 2000, Fig. 2.11; supplement, p. 300-301), often associated with the injection of clastic material, features atypical of Beacon strata in outcrop along the TAM. In addition,

“The deformation is therefore likely to be due to rift-related down-faulting along the Transantarctic Mountain Front. This brecciation and mobilisation may have been associated with intrusion-related hydrothermal activity” (Cape Roberts Science Team, 2000, p. 200).

We recorded a rather isolated abundance maximum of radial authigenic smectite in three consecutive samples between 533.26 and 550.03 mbsf (Tab. 1), which spans the brittle fault at 539 mbsf (Fig. 2). Around this same interval, Ehrmann (this volume) recorded at 542.7 and 551.7 mbsf anomalously high percentages of smectite measured against an internal standard. This he attributed to diagenetic processes along the hydrologically active fault.

A major candidate for past hydrothermal activity in CRP-3 is the highly altered intrusion in the Beacon (Unit 17.1). If it was emplaced and altered during the Devonian, however, it is not relevant to our current problem. If it is of Devonian age but was altered by hydrothermal fluids or burial diagenesis during the Oligocene, then it may have contributed cations for smectite precipitation in the Cenozoic section provided those fluids could reach the younger sediments. Hydrothermal fluids might have moved upward along a fault. It is difficult to envision, however, how fluids could have moved upward during burial diagenesis because the overlying Beacon sandstones, although porous and permeable, seem to be devoid of authigenic smectite, except possibly immediately above the intrusion where some discoloration was noted in the sandstone (Cape Roberts Science Team, 2000). It would be much easier to establish a case for hydrothermal activity if the intrusion were emplaced during the Oligocene. As yet, however, its date of emplacement is unknown.

Another candidate to indicate hydrothermal activity might be the dolerite breccia within the shear zone at 790-806 mbsf, which immediately underlies the Cenozoic marine sequence. As discussed previously, however, both the present-day intergranular and fracture permeabilities appear to be low in this fault zone. Secondly, as discussed above, the

extremely negative oxygen-isotopic values recorded in carbonate within the sandstones immediately above at 787.84 mbsf are best interpreted as being indicative of low-temperature mixing of meteoric waters rather than high-temperature hydrothermal fluids.

It is worth exploring, however, the possibility that hydrothermal fluids at some later stage after smectite authigenesis might be responsible for the presence of the extensive carbonate cements that pervade the central portion of CRP-3 (c. 225-625 mbsf; see Tab. 1 and Dietrich et al., this volume). Calcite filling of fractures is common in this interval and in both the 257-263 and 539 mbsf faults. The focused injection of carbonate-rich hydrothermal fluids along such fault planes such as that at 257-263 mbsf might explain why only the middle portion of the Oligocene section is pervasively carbonate cemented. As Pittman et al. (1992) pointed out, the presence of clay coats does not affect the precipitation of carbonate cements, which is certainly the case at CRP-3.

No other obvious source of carbonate has yet been found for the calcite cements in CRP-3 below 300 mbsf as calcareous micro- and macro-fossils are now, and apparently have always been, rare or absent throughout this portion of the core. The lack of appreciable organic matter in the section (Kettler, this volume) would tend to rule out methanogenic carbonate precipitation. On the other hand, the occurrence of marble in the Cambrian/Precambrian metamorphic complex that underlies the Beacon Supergroup in this region could provide a suitable carbonate source if these were mobilized by circulating fluids of some acidity.

A clast of graphite-bearing marble was logged at 337.57 mbsf (Cape Roberts Science Team, 2000, Tab. 4.1), which was attributed to the amphibolite-facies Koettlitz Group that crops out south of the Mackay Glacier (Cape Roberts Science Team, 2000, and references therein). The Koettlitz Group is intruded by the Granite Harbour Igneous Complex, which crops out in the Cape Roberts/Mackay Glacier area. Thus, a single clast, which could have been rafted in from the south, is by no means proof of its occurrence in the basement beneath the CRP-3.

Nevertheless, a general modern analog for the carbonate cementation at CRP-3 might be the deposition of travertine at Minerva Terrace (Mammoth Hot Springs) in Yellowstone National Park (USA), which is sourced by hot, presumably acidic solutions moving through Pennsylvanian limestones (Ruppel, 1972; Tuttle, 1990). Although this is a vastly larger system operating over a much longer period of time than any at CRP3, this example does illustrate the potential that hot fluids can have in mobilizing calcium carbonate.

At CRP-3 any such solutions apparently did not reach the surface in the study area. However, scavenging of carbonate from marbles in metamorphic basement terranes by hot solutions would be a

possible mechanism for sourcing the copious amounts of carbonate cement found within the core.

### **A case for smectite emplacement by fault-focused compactional fluids**

There is a fault bounding a large graben just west of CRP-3 (Fig. 2). As summarized by Burley and MacQuaker (1992; see references therein), such faults can be conduits for compactional fluids from deeper reservoirs (“thermobaric” fluids) and, during times of fault displacement, can actively pump or valve fluids. By these mechanisms, large volumes of fluids can be moved rapidly from one formation to another either across faults or along their planes. Pressure decrease and fluid cooling may result in the precipitation of clay minerals and authigenic quartz. On the other hand, dissolution of detrital and authigenic components may occur in the case of minerals with retrograde solubilities, such as calcite, as a result of cooling (Giles & de Boer, 1989). Burley & MacQuaker (1992) reported evidence of fault-related fluid flow and diagenetic modification in many North Sea Jurassic reservoir sandstones. They found that the...

“concentration of cementation adjacent to faults and at crests of structures, the presence of temperature anomalies from fluid inclusions and the cyclical nature of cementation all suggest that faults exert a major influence on deep subsurface diagenesis by controlling fluid flow, fluid mixing and localization of cements and porosity enhancement” (Burley & MacQuaker, 1992, p. 104).

These authors present a conceptual model of fault-related fluid movement driven by compactional fluid flow in which regional compactive “thermobaric” fluids are channeled upward along a fault plane (Burley & MacQuaker, 1992, Fig. 28) before being injected into a porous reservoir undergoing dilation. In such a case, the most intense diagenesis would occur just beneath a “seal” over the sand body. Other authors have pointed out limitations with such a model, however, and contend that the effects from such fault-focusing of fluids “cannot be invoked except to explain local phenomena” (Bjørlykke & Aagaard, 1992).

Such a model, however, might be applicable to the situation at CRP-3 in view of the boundary fault thought to lie just west of the site (Fig. 1). Fluids generated at depth in a down-thrown sedimentary section may have been injected along this fault during graben development shortly after the Oligocene sediments at CRP-3 had been deposited. Seismic interpretation suggests that the age of the material in the down-thrown section would likely be early Oligocene (possibly latest Eocene) (Seismic sequence V5; Fig. 1). The graben may also harbor Seismic sequence V6, which is thought to include in part the McMurdo Volcanic Group (upper Oligocene to Holocene) as well as yet unsampled Palaeogene early rift volcanic rocks or possibly the Mesozoic Ferrar

Supergroup (Cape Roberts Science Team, 2000, Figs. 7.7 and 7.8).

As discussed previously the character of the sediments in CRP-3 changes upsection at 380 mbsf, where “well-sorted clean sands become rare and are replaced by muddy sands and mud, diamictites and conglomerates become more prominent upcore (Lithofacies Association 5)” (Cape Roberts Team, 2000). The muddier sediments, which have considerably reduced permeabilities (Fig. 7), could have retarded the upward movement of “thermobaric” fluids, effectively functioning as the “seal” in the model of Burley & MacQuaker (1992). This might explain why we noted the last consistent occurrence of authigenic smectites at 351.88 mbsf and the last actual occurrence at 335.96 mbsf (Tab. 1). This would also explain the absence of such precipitates in the base of CRP-2, which lies farther to the east of the fault and farther upsection (Fig. 2). It would also allow for a short-term, one-shot emplacement, which would be in keeping with the single generation of cementation observed.

## **SUMMARY AND CONCLUSIONS**

The existence of authigenic smectite in CRP-3 is confirmed. It was emplaced as a single generation of cementation within marine sandstones in the lower portion of the Oligocene section that has undergone no discernible compaction since carbonate cementation.

We have made a case for the precipitation of smectite during burial diagenesis with necessary components sourced from volcanogenic materials and heavy minerals within the drilled sequence. We have also made a case for precipitation from hydrothermal waters associated with possible igneous intrusion(s) and nearby faults. Last we have examined a model involving the mobilisation of regional compactive “thermobaric” fluids along a fault.

These models are submitted here as multiple working hypotheses to be tested by further research. The most straightforward of these three models is the first discussed: that smectite authigenesis occurred during burial diagenesis. Meteoric waters may have played a role in this scenario. This model (our Case No. 1) is favored in that all of the necessary conditions seem to have been met for smectite authigenesis and, in comparison with the others presented, it is the least complicated, (*i.e.* Occum’s razor is applicable here). The other models require special circumstances and events that are not only more complicated, but which need to be independently documented. Because our drill holes were situated on the margin of a rapidly subsiding rift basin, however, special circumstances might apply.

Of these other scenarios, we consider the hydrothermal model (our Case No. 2) the most likely of the two in that there is evidence of strong

alteration of a dolerite sill in the Beacon sandstone, the timing of which, however, is yet unknown. There also may be a suggestion of hydrothermal emplacement or diagenetic alteration associated with a fault at 539 mbsf. Case No. 3 is based on a largely untested model from the North Sea, about which there has been considerable debate and discussion (compare Burley & MacQuaker, 1992, and Bjørlykke & Aagaard, 1992).

Considerably more work needs to be done, however, to better arbitrate between these possible models for smectite authigenesis. Required as a minimum are more analyses via the SEM to confirm the total extent of the authigenic smectite in the Cape Roberts cores. Equally important is the need for radiometric age dates on the clay minerals in both the sandstones and the intrusive body. Other important unknowns in our understanding at this point are details of the general structural history of the study area and that of the graben to the west of CRP-3. The structure of the graben is apparently not simple and straightforward as it is broken by additional subvertical faults, and seismic sequence V6 may or may not be present there.

As the reader will readily appreciate, this current study has answered some questions about the nature of authigenic mineral phases in CRP-3, but on the other hand has raised other questions that cannot be answered at present. This paper, therefore, is titled at this point a "progress report".

**ACKNOWLEDGMENTS** - We thank our Cape Roberts Team colleagues for many stimulating discussions, for making available their unpublished data/observations, as well as for their good company "on the ice". Dr. Edward D. Pittman provided helpful information and comments on an early draft of the manuscript, which was further improved by critical and editorial reviews by Drs. Mary Anne Holmes and Malcolm Laird, respectively. Kim Riddle skillfully operated the SEM, and David Davenport drafted/composed many of the figures. Support for SWW was provided by NSF grant OPP-9433893, for RDJ by OPP-9418429, and for LK by OPP-9527008.

#### REFERENCES

Aghib F.S., Claps M. & Sarti M., 2000. Preliminary report on the main carbonate diagenetic features of the Oligocene strata from CRP-2/2A, Victoria Land Basin, Antarctica. *Terra Antartica* **7**, 393-400.

Almon W.R., Fullerton L.B. & Davies D.K., 1976. Pore space reduction in Cretaceous sandstones through chemical precipitation of clay minerals. *Journal of Sedimentary Petrology*, **46**, 89-96.

Barrett P.J., 2001. Grain-size analysis of samples from Cape Roberts Core CRP-3, Victoria Land Basin, Antarctica, with inferences about depositional setting and environment. This volume

Biscaye P.E., 1965. Mineralogy and sedimentation of recent deep-sea clay in the Atlantic Ocean and adjacent seas and oceans. *Bulletin of the Geological Society of America*, **76**, 803-832.

Bjørlykke K. & Aagaard P., 1992. Clay minerals in North Sea sandstones. In: Houseknecht D.W. & Pittman E.D. (eds.), *Origin, Diagenesis, and Petrophysics of Clay Minerals in*

*Sandstones*, SEPM Special Publication, **47**, 65-80.

Bohrmann G., Abelmann A., Geresonde R., Hubberten H. & Kuhn G., 1994. Pure siliceous ooze, a diagenetic environment for early chert formation. *Geology*, **22**, 207-210.

Brink J.D. & Jarrard R.D., 2000. Petrophysics of core plugs from CRP-2/2A drillhole, Victoria Land Basin, Antarctica. *Terra Antartica*, **7**, 231-240.

Brink J.D., Jarrard R.D., Bucker C., Wonik T. & Talarico F., 2000. Sedimentological interpretation of Well Logs from CRP-2/2A, Victoria Land Basin, Antarctica: glacial and sea-level significance. *Terra Antartica*, **7**, 349-360.

Bucker C.J., Jarrard R.D., Niessen F. & Wonik T., 2001. Statistical analysis of wireline logging data of the CRP-3 drillhole, Victoria Land, Antarctica. This volume.

Burley S.D. & MacQuaker, J.H.S., 1992. Authigenic clays, diagenetic sequences, and conceptual diagenetic models in contrasting basin-margin and basin-center North Sea Jurassic sandstones and mudstones. In: Houseknecht D.W. & Pittman E.D. (eds.), *Origin, Diagenesis, and Petrophysics of Clay Minerals in Sandstones*, SEPM Special Publication, **47**, 81-110.

Cape Roberts Science Team, 1998. Initial Report on CRP-1, Cape Roberts Project, Antarctica. *Terra Antartica*, **5**, 1-187.

Cape Roberts Science Team, 1999. Studies from the Cape Roberts Project, Ross Sea, Antarctica. Initial Report on CRP-2/2A. *Terra Antartica*, **6**, 1-173. With Supplement, 245 p.

Cape Roberts Science Team, 2000. Studies from the Cape Roberts Project, Ross Sea, Antarctica. Initial Report on CRP-3. *Terra Antartica*, **7**, 1-208. With Supplement, 305 p.

Chamley H., 1989. *Clay Sedimentology*. Springer, Berlin, 623 p.

Craig H., 1965. The measurement of oxygen isotope palaeotemperatures. *Proceedings of the Spoleto Conference on Stable Isotopes, Oceanographic Studies, and Palaeotemperatures*, 1965, 1-24.

Daniel L.M.F., Souza E. M. & Mato L.F., 1989. Geoquímica e modelos de migração de hidrocarbonetos no Campo de Rio do Buitengração com o compartimento nordeste da Bacia do Recôncavo, Bahia. *Boletim de Geociências da Petrobras*, **3**, 159-169.

Davies D.F. & Almon W.R., 1979. Reservoir Potential of volcanogenic sandstones, *Bulletin of the American Association of Petroleum Geologists*, **63**, 843.

Davies D.F., Almon W.R., Bonis S.B. & Hunter B.E., 1979. Deposition and diagenesis of Tertiary-Holocene volcanoclastics, Guatemala. In: Scholle P.A. & Schluger P.R. (eds.), *Aspects of Diagenesis*, SEPM Special Publication, **26**, 281-306.

Diekmann B., Petschick R., Gingele F.X., Fütterer D.K., Abelmann A., Brathauer U., Gersonde R. & Mackensen A., 1996. Clay mineral fluctuations in Late Quaternary sediments of the southeastern South Atlantic: implications for past changes of deep water advection. In: Wefer G., Berger W.H., Siedler G. & Webb D.J. (eds.), *The South Atlantic: present and past circulation*. Springer, Berlin, 621-644.

Dietrich H.-G., Klosa D. & Wittich C., 2001. Carbonate content in CRP-3 drillcore, Victoria Land Basin, Antarctica. This volume.

Eberl D.D. & Hower J., 1976. Kinetics of illite formation. *Geological Society of America Bulletin*, **87**, 1326-1330.

Ehrmann W.U., 1997. Smectite concentrations and crystallinities: indications for Eocene Age of Glaciomarine sediments in the CIROS-1 Drill Hole, McMurdo Sound, Antarctica. In: Ricci C.A. (ed.), *The Antarctic Region: Geological Evolution and Processes*, Terra Antartica Publication, Siena, 771-780.

Ehrmann W.U., 1998a. Implications of late Eocene to early Miocene clay mineral assemblages in McMurdo Sound (Ross Sea, Antarctica) on palaeoclimate and ice dynamics. *Palaeogeography, Palaeoclimatology, and Palaeoecology*, **139**, 213-231.

Ehrmann W.U., 1998b. Lower Miocene and Quaternary clay mineral assemblages from CRP-1. *Terra Antartica*, **5**, 613-619.

Ehrmann W.U., 2000. Smectite content and crystallinity in sediments from CRP-2/2A, Victoria Land Basin, Antarctica. *Terra Antartica*, **7**, 575-580.

Ehrmann W.U., Melles M., Kuhn G. & Grobe H., 1992. Significance of clay mineral assemblages in the Antarctic Ocean. *Marine Geology*, **107**, 249-273.

Florindo F., Wilson G.S., Roberts A.P., Sagnotti L. & Verosub K.L., 2001. Magnetostratigraphy of late Eocene - early Oligocene strata from the CRP-3 core, Victoria Land Basin, Antarctica. This volume.

- Giles M.R. & de Boer R.B., 1989. Secondary porosity: creation of enhanced porosities in the subsurface from the dissolution of carbonate cements as a result of cooling formation waters. *Marine and Petroleum Geology*, **6**, 261-269.
- Gluyas J. & Oxtoby N., 1995. Diagenesis: a short (2 million year) story- Miocene sandstones of central Sumatra, Indonesia. *Journal of Sedimentary Research*, **A65**, 3-31.
- Griffin J.J., Windom H. & Goldberg E.D., 1968. The distribution of clay minerals in the World Ocean. *Deep-Sea Research*, **15**, 433-459.
- Hannah M.J., Wrenn J.H. & Wilson G.J., 2001. Preliminary report on early Oligocene and ?latest Eocene marine palynomorphs from CRP-3 drillhole, Victoria Land Basin, Antarctica. This volume.
- Hamilton E.L., 1976. Variations of density and porosity with depth in deep-sea sediments. *Journal of Sedimentary Petrology*, **46**, 280-300.
- Harwood D.M. & Webb P.-N., 1998. Glacial Transport of diatoms in the Antarctic Sirius Group: Pliocene refrigerator. *GSA Today*, **8**, 4-8.
- Harwood D.M. & Bohaty S., 2001. Early Oligocene siliceous microfossil biostratigraphy of Cape Roberts Project core CRP-3, Victoria Land Basin, Antarctica. This volume.
- Hathon L.A. & Houseknecht D.W. Origin and diagenesis of clay-minerals in the Oligocene Sespe Formation, Ventura Basin. In: Houseknecht D.W. & Pittman E.D. (eds.), *Origin, Diagenesis, and Petrophysics of Clay Minerals in Sandstones*, SEPM Special Publication, **47**, 185-195.
- Houseknecht D.W. & Pittman E.D. (eds.), *Origin, Diagenesis, and Petrophysics of Clay Minerals in Sandstones*, SEPM Special Publication, **47**, 282 p.
- Jarrard R., 2001. Petrophysics of core plugs from CRP-3 drillhole, Victoria Land Basin, Antarctica. This volume.
- Khoury H.N. & Eberl D.D., 1979. Bubble-wall shards altered to montmorillonite. *Clays and Clay Minerals*, **27**, 291-292.
- Kettler R.M., 2001. Results of whole-rock organic geochemical analyses of the CRP-3 drillcore, Victoria Land Basin, Antarctica. This volume.
- Kyle P.R., 1998. Ferrar dolerite clasts from CRP-1 drillcore. *Terra Antarctica*, **5**, 611-612.
- LeBas M.J., LeMaitre R.W., Streckeisen A. & Zanettin B., 1986. A chemical classification of volcanic rocks based on the total alkali-silica diagram. *Journal of Petrology*, **27**, 745-750.
- Lerbekmo J.P., 1957. Authigenic montmorillonoid cement in andesitic sandstones of central California. *Journal of Sedimentary Petrology*, **27**, 298-305.
- Lombardi G. & Mattias P., 1981. *Guidebook for the Excursions in Sardinia and Central Italy*, 7<sup>th</sup> International Clay Conference, Istituto Poligrafico e Zecca dello Stato P.V., Roma, 80-90.
- McKenzie D.P., 1978. Some remarks on the development of sedimentary basins. *Earth and Planetary Science Letters*, **40**, 25-32.
- Miller M.F. & Mabin M.C.G., 1998. Antarctic Neogene landscapes - In the refrigerator or the deep freeze?, *GSA Today* **8**, 1-3.
- Moraes M.A.S. & De Ros L.F., 1992. Depositional, infiltrated and authigenic clays in fluvial sandstones of the Jurassic Sergi Formation, Recôncavo Basin, northeastern Brazil. In: Houseknecht D.W. & Pittman E.D. (eds.), *Origin, Diagenesis, and Petrophysics of Clay Minerals in Sandstones*, SEPM Special Publication, **47**, 197-208.
- Nelson P.H., 1994. Permeability-porosity relationships in sedimentary rocks, *Log Analyst*, **35**, 38-62.
- Neumann M. & Ehrmann W., 2001. Mineralogy of Sediments from CRP-3 as Revealed by X-Ray Diffraction. This volume.
- Niessen F., Jarrard R.D. & Bucker C., 1998. Log-based physical properties of the CRP-1 Core, Ross Sea, Antarctica. *Terra Antarctica*, **5**, 299-310.
- Pompilio M., Armienti P. & Tamponi M., 2001. Petrography, mineral composition and geochemistry of volcanic and subvolcanic rocks of CRP-3, Victoria Land Basin, Antarctica. This volume.
- Odin G.S., 1988. Glaucony from the Gulf of Guinea. In: Odin G.S. (ed.), *Green Marine Clays*, Developments in Sedimentology **45**, Elsevier, Amsterdam, 225-275.
- O'Neil J.R., Clayton, R. N., & Mayedo, T.K., 1969. Oxygen isotope fractionation in divalent metal carbonates. *Journal of Chemical Physics*, **51**, 5547-5558.
- Pittman E.D., Larese R.E. & Heald M.T., 1992. Clay coats: occurrence and relevance to preservation of porosity in sandstones. In: Houseknecht D.W. & Pittman E.D. (eds.), *Origin, Diagenesis, and Petrophysics of Clay Minerals in Sandstones*, SEPM Special Publication, **47**, 241-255.
- Pompilio M., Armienti P. & Tamponi M., 2001. Petrography, Mineral Composition and Geochemistry of Volcanic and Subvolcanic Rocks of CRP-3. This volume.
- Ruppel E.T., 1972. Geology of the pre-Tertiary rocks in the northern part of Yellowstone National Park. *U.S. Geological Survey Professional Paper*, **729**, A1-A66.
- Sagnotti L., Verosub K.L., Roberts A.P., Florindo F. & Wilson G.S., 2001. Environmental magnetic record of the Eocene-Oligocene transition in CRP-3 drillcore, Victoria Land Basin, Antarctica. This volume.
- Sandroni S. & Talarico F., 2001. Petrography and Provenance of Basement Clasts and Clast Variability in CRP-3 Drillcore (Victoria Land Basin, Ross Sea, Antarctica). This volume.
- Scholle P.A. & Schluger P.R. (eds.), 1979. *Aspects of Diagenesis*, SEPM Special Publication, Tulsa, Oklahoma USA, **26**, 443p.
- Setti M., Marinoni L. & Lopez-Galindo A., 2001. Crystal-chemistry of smectites in sediments of CRP-3 drillcore (Victoria Land Basin, Antarctica): preliminary results. This volume.
- Small J.S., Hamilton D.L. & Habesch S., 1992a. Experimental simulation of clay precipitation within reservoir sandstones 1: techniques and examples. *Journal of Sedimentary Petrology*, **62**, 508-519.
- Small J.S., Hamilton D.L. & Habesch S., 1992b. Experimental simulation of clay precipitation within reservoir sandstones 2: Mechanism of illite formation and controls on morphology. *Journal of Sedimentary Petrology*, **62**, 520-529.
- Smellie J., 2000. Erosional history of the Transantarctic Mountains deduced from sand grain detrital modes in CRP2/2A, Ross Sea, Antarctica. *Terra Antarctica* **7**, 545-552.
- Smellie J., 2001. History of Oligocene Erosion, Uplift and Unroofing of the Transantarctic Mountains Deduced from Sandstone Detrital Modes in CRP-3 Drillcore, Ross Sea, Antarctica. This volume.
- Spötl C., Houseknecht D.W. & Longstaffe F.J., 1994. Authigenic chlorites in sandstones as indicators of high-temperature diagenesis, Arkoma foreland basin, USA. *Journal of Sedimentary Research*, **A64**, 553-566.
- Stanley K.O. & Benson L.V., 1979. In: Scholle P.A. & Schluger P.R. (eds.), *Aspects of Diagenesis*, SEPM Special Publication, **26**, 401-423.
- Stroeven A.P., Burckle L.H., Kleman J. & Prentice M.L., 1998. Atmospheric transport of diatoms in the Antarctic Sirius Group: Pliocene Deep Freeze. *GSA Today*, **8**, 4,5.
- Sturesson U., 1992. Volcanic ash: the source material for Ordovician chamosite ooids in Sweden. *Journal of Sedimentary Petrology*, **62**, 1084-1094.
- Surdam R.C. & Boles, J.R., 1979. Diagenesis of volcanic sandstones. In: Scholle P.A. & Schluger P.R. (eds.), *Aspects of Diagenesis*, SEPM Special Publication, **26**, 227-242.
- Thorez J., 1976. *Practical identification of clay minerals*. Dison, 80 p.
- Thorn V.C., 2001. Oligocene and early Miocene phytoliths from CRP-2/2A and CRP-3, Victoria Land Basin, Antarctica. This volume.
- Tuttle S.D., 1990. Yellowstone National Park. In: Harris, A.G. & Tuttle, E.(eds.), *Geology of National Parks, 4<sup>th</sup> Edition*, Kendall/Hunt Publ. Co., Dubuque, 490-500.
- Watkins D.K., Wise S.W., Jr. & Villa G., 2001. Calcareous nannofossils from Cape Roberts Project drillhole CRP-3, Victoria Land Basin, Antarctica. This volume.
- Whitney G., 1990. Role of water in the smectite-to-illite reaction. *Clays and Clay Minerals*, **38**, 343-350.
- Wilson M.D. & Pittman E.D., 1977. Authigenic clays in sandstones: recognition and influence on reservoir properties and palaeoenvironmental analysis. *Journal of Sedimentary Petrology*, **47**, 3-31.
- Wise S.W. & Ausburn M.P., 1980. Kinney bentonite: re-examined. *SEM/1980/I*, SEM Inc., AMF O'Hare, 565-571.
- Wise S.W. & Weaver F.M., 1979. Volcanic ash: example of devitrification and early diagenesis. *SEM/1979/I*, SEM Inc., AMF O'Hare, 511-518.